Magnetotransport properties of a uniaxially compressed 2D electron gas at a grain boundary of $Hg_{1-x}Cd_xTe$ ($x=0.23$) bicrystals

N. B. Butko, N. Ya. Minina, and A. M. Savin
Physics Faculty, M. V. Lomonosov Moscow State University, 119899 Moscow, Russia

W. Kraak and S. Krause
Physical Institute of Humboldt University, D-10115 Berlin, FRG

(Submitted 26 April 1994)
Pis'ma Zh. Eksp. Teor. Fiz. **59**, No. 11, 760–764 (10 June 1994)

Quantum oscillations of the magnetoresistance of 2D electrons in an inversion layer at the interface of p-$Hg_{1-x}Cd_xTe$ ($x=0.23$) bicrystals have been studied during hydrostatic compression to $P=8$ kbar and during uniaxial compression with $\sigma_{yy}=1.5$ kbar in the direction perpendicular to the 2D layer. The oscillation frequency F_i and correspondingly the density n_i of the 2D electrons in each of the three observed energy subbands in the quantum well increase during the uniaxial compression. This change is opposite to the change observed during the hydrostatic compression, at which the n_{si} in all subbands fall off rapidly with the pressure, so that the inversion layer disappears at $P>10$ kbar.

Two dimensional (2D) inversion layers of charge carriers at grain boundaries of semiconductor bicrystals, e.g., in p-InSb (Ref. 1), p-$He_{1-x}Mn_xTe$ (Ref. 2), n-Ge (Ref. 3), and p-HgCdTe (Ref. 4), are currently the subject of active and successful research. These 2D systems, which arise naturally in the course of crystal growth, in contrast with heterostructures created artificially at the surface of semiconductors, are in the interior of the sample and are ideal entities for studying the role played by the energy spectrum and crystal structure of the bulk material in shaping the potential well and properties of the 2D charge carriers. From this standpoint, it is extremely promising to study the magnetotransport properties of 2D electron inversion layers at grain boundaries of bicrystals during a deformation of the crystal lattice which changes the band structure and properties of the energy spectrum of the bulk crystal adjacent to the 2D layer.

In this paper we are reporting a study of the Shubnikov–de Haas effect, the resistance, and the Hall effect in a quantum well at a grain boundary of a bicrystal of a narrow-gap p-$Hg_{1-x}Cd_xTe$ ($x=0.23$) semiconductor with a direct gap $E_g=90$ meV and an uncompensated-acceptor concentration $N_A-N_D=10^{15}$ cm^{-3} during uniaxial compression at loads up to 1.5 kbar. The effect of hydrostatic compression on the properties of the electrons in the inversion layer of such samples was studied in Ref. 5. It was found that an increase in the pressure P causes a pronounced decrease in the population n_i in all three observed subbands. At $P>10$ kbar, the effect is the complete disappearance of the inversion layer.

The samples, with dimensions of $1\times0.5\times3$ mm, were subjected to uniaxial compression at loads up to 1.5 kbar by the method of Ref. 6. The compression direction was

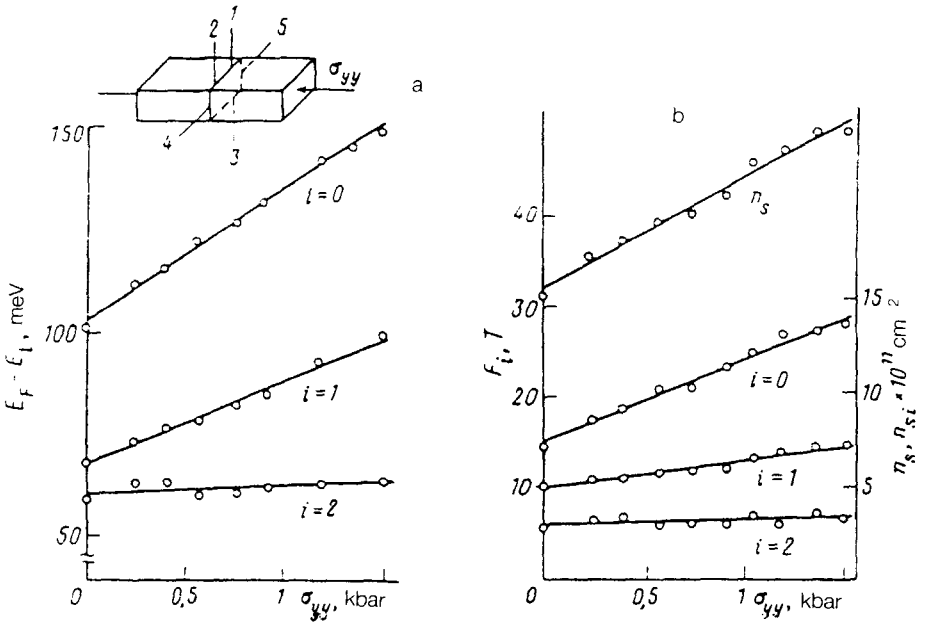

FIG. 1. Deformation dependence of the characteristic energies $\Delta E_i = E_F - E_i$ (a), the frequencies of the Shubnikov–de Haas oscillations F_i (left scale) and carrier density n_{si} (right scale) (b) in each of the subbands in the inversion layer at the grain boundary of the p-$He_{1-x}Cd_xTe$ bicrystal. Here n_s is the total density of carriers. The inset shows the arrangement of contacts on the sample. *1,2*—Potential contacts; *1,3*—Hall contacts; *4,5*—current contacts.

perpendicular to the grain boundary. The direction of the relief stress σ makes an angle $\approx 30°$ with the [110] direction, 51° with [111], and 14° with [100]. The arrangement of the current, potential, and Hall contacts at the boundary of the grains of the bicrystal is shown in the inset in Fig. 1a. The potential and Hall contacts were welded to the grain boundary with a gold wire 25 μm in diameter by an electric-arc method or by means of drops of the alloy In+3%Au with an area $\sim(1-2)\times 10^{-2}$ mm^2. Current contacts were soldered in the form of a thin strip of the alloy InAu distributed along the grain boundary. At liquid-helium temperature the resistance of the bulk part of the crystal was several tens of times the resistance at the grain boundary. This relation ruled out a shunting of the signal by the interior of the sample.

The 2D properties of the inversion layer at a grain boundary are manifested primarily in the presence of clearly expressed quantum oscillations of the magnetoresistance. Their frequency F is given by $F(\varphi) = F_0 \cdot \cos\varphi$, where φ is the angle between the magnetic field **H** and the normal to the grain boundary. This angular dependence for the frequency is characteristic of 2D electrons. In the 3D p-$He_{1-x}Cd_xTe$ crystal ($E_g \geq 90$ meV), the magnetoresistance is of course a monotonic function.

When a uniaxial stress σ is applied, there is a pronounced increase in the frequencies of the Shubnikov–de Haas oscillations F_i corresponding to the two lower subbands in the quantum well at the p-$He_{1-x}Cd_xTe$ grain boundary (Fig. 1) ($\Delta F_0/F_0 \approx 100\%$ for

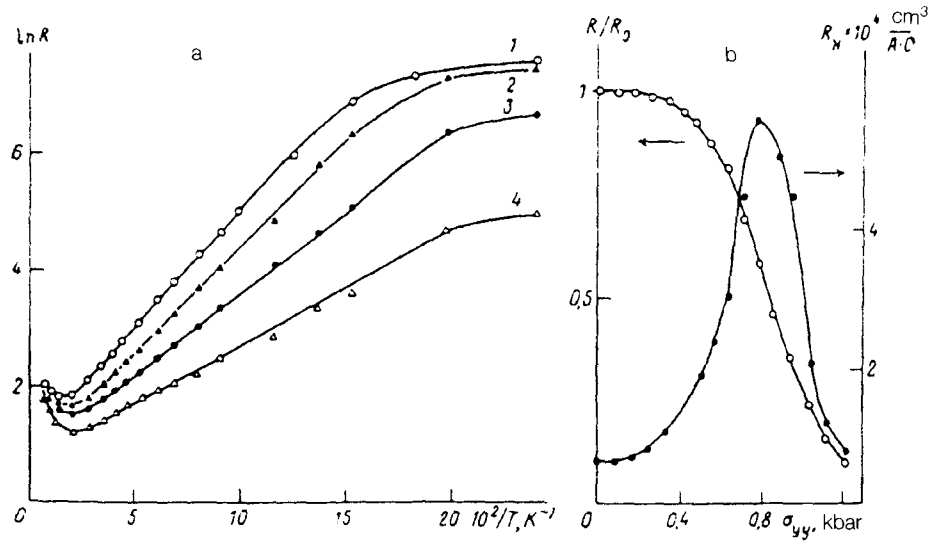

FIG. 2. (a) Temperature dependence of the resistance at various values of the deformation. (b) Deformation dependence of the Hall coefficient (scale at right) and of the relative resistance (scale at left). *1*—$\sigma_{yy}=0$ kbar, $\epsilon_A=3.5$ meV; *2*—$\sigma_{yy}=0.5$ kbar, $\epsilon_A=2.9$ meV; *3*—$\sigma_{yy}=0.9$ kbar, $\epsilon_A=2.4$ meV; *4*—$\sigma_{yy}=1.2$ kbar, $\epsilon_A=1.7$ meV.

$\sigma_{yy}=1.5$ kbar). For the highest subband, the change in the frequency F_2 is no greater than the error in its determination, $\Delta F_2/F_2 \approx 2\%$. The carrier densities in the subbands, $n_{si}=e/[\pi h \Delta_i(1/B)]$ cm^{-2}, are calculated, where $\Delta_i(1/B)$ is the corresponding period of the quantum oscillations (Fig. 1b). The characteristic energies of the subbands, $\Delta E_i=E_F-E_i$, are also calculated (Fig. 1a). The calculation of ΔE_i was carried out in the Kane model with effective masses corresponding to the bulk part of the sample. The total density of 2D carriers in the inversion layer, $n_s=\Sigma n_{si}$, increases sharply with increasing σ, as does ΔE_i in the two lower subbands (Fig. 1). This result is qualitatively opposite the effect observed during hydrostatic compression.[5] The increase in n_s is in agreement with the decrease in the resistance R observed during uniaxial compression (a decrease of 30% at $\sigma_{yy}=1.2$ kbar) and in the Hall coefficient R_H (by 20% at $\sigma_{yy}=1.2$ kbar).

Figure 2 shows the data from control measurements of the deformation dependence of R, R_H, and $R(T)$ of bulk p-$Hg_{1-x}Cd_xTe$ samples cut from various regions of the ingot near the bicrystal grain boundary under study. The fundamental difference between the effect of the anisotropic (uniaxial) deformation from the effect of hydrostatic compression on the energy spectrum of bulk p-$Hg_{1-x}Cd_xTe$ crystals is a change in the symmetry of the crystal lattice and a lifting of the symmetry-induced degeneracy of the valence band in Γ_8. Its splitting into heavy- and light-hole band increases rapidly with the deformation, reaching 12 meV and $\sigma \approx 1$ kbar (Ref. 7). The magnitude of the direct energy gap E_g, according to the temperature dependence of the resistance increases much more slowly than during hydrostatic compression: $\partial E_g/\partial\sigma \approx 4.3$ meV/kbar (according to the present study) versus $\partial E_g/\partial\sigma=5$ meV/kbar (Ref. 8).

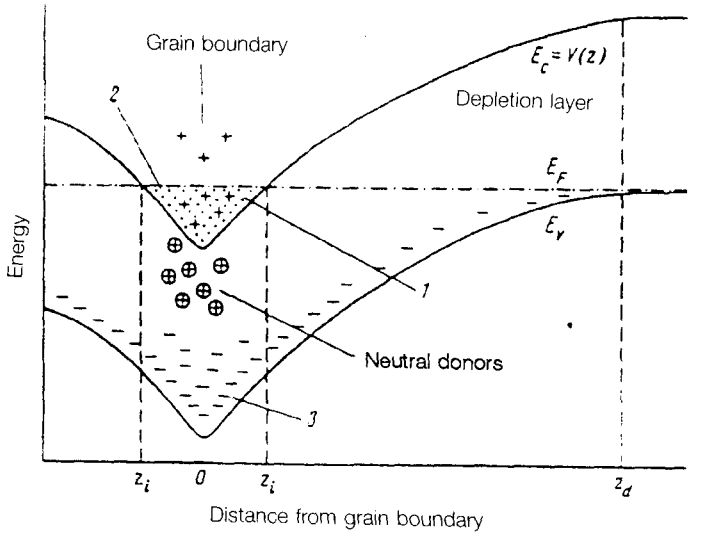

FIG. 3. Charge distribution near the grain boundary of bicrystals of a p-type semiconductor when there is an inversion layer at the boundary ($z=0$). *1*—Charged donor states; *2*—electrons in inversion layer; *3*—charged acceptor states.

The activation energy ϵ_A of the acceptor level near the top of the valence band, which apparently does not change during hydrostatic compression,[9] decreases in the case of uniaxial compression: $\partial\epsilon_A/\partial\sigma = 1.6$ meV/kbar (Fig. 2a), $\partial\epsilon_A/\partial\sigma = 2.2$ meV/kbar (Ref. 7). The decrease in the resistance $R(\sigma)$ and the peak on the deformation curve of the Hall coefficient, $R_H(\sigma)$ (Fig. 2b) [a similar peak has been observed previously[7,8] on the temperature curves $R_H(T)$], indicates that a change in the conduction mechanism occurs at 4.2 K in the interior of p-$He_{1-x}Cd_xTe$ samples in the course of uniaxial compression ($\sigma \approx 0.7$ kbar). The change is from a conduction through an impurity acceptor band to a conduction by free holes in the upper extremum of the extrema that were split in the valence band. The latter circumstance may affect a redistribution of charges near the potential barrier at the grain boundary of the bicrystals.

Qualitative and quantitative analyses of charge states at grain boundaries which lead to the appearance of a potential barrier were carried out in Ref. 10 for p-InSb bicrystals. Since the crystalline band structures of p-InSb and p-$Hg_{1-x}Cd_xTe$ with $x > 0.16$ and $E_g > 0$ are identical, the results of Ref. 10 and the approach developed in the present study to interpret the observed effects are completely applicable to p-$He_{1-x}Cd_xTe$ of the composition under study. An important point is that we are dealing with three types of states, localized near the grain boundary and distributed over a fairly broad energy range (curves 1–3 in Fig. 3), while the hole concentration $p(z)$ in the region in which the potential barrier $V(z)$ exists is assumed to be zero. According to Ref. 10, positively charged states *1* are associated with the formation of ruptured bonds and other dislocations at the grain boundary, while negatively charged states correspond to acceptor impurities segregated at the boundary. A self-consistent calculation of $V(z)$ was carried out in Ref. 10 on the basis of a solution of the Poisson equation with electrical neutrality. The

result shows that in the model adopted for the distribution of charges a hydrostatic compression does not lead to a further curvature of the band boundaries [the potential barrier $V(z)$ is not affected by the pressure]. A decrease in the density of 2D electrons is caused exclusively by an increase in the energy gap in the 3D part of the sample, at a rate $\partial E_g/\partial P = 15$ meV/kbar (Ref. 11). This increase leads to a shift of the bottom of the band with respect to the Fermi level at approximately the same rate,[6] $\partial V/\partial P = 15.5$ meV/kbar.

An increase in the number of free holes in the interior of the sample during uniaxial compression may lead to a disruption of the charge equilibrium which exists near the grain boundary at $\sigma_{yy}=0$. It may also lead to the appearance of additional negative charge near the boundary of the bicrystal. Such a charge can arise in the scheme shown in Fig. 3, if the bottom of the potential well becomes lower with respect to the Fermi level (Fig. 1a) and if there is a corresponding increase in the electron density n_s in the inversion layer (Fig. 1b). At the observed small increase in the width of the band gap E_g with increasing uniaxial deformation, this picture suggests an increase in the height of the potential barrier at the grain boundary and requires a special calculation. It may also be necessary to consider the probability for piezoelectric effects in crystals with the zinc blende structure, since they do not have a symmetry center. However, it is clear even at this stage that the band structure and the crystal lattice of the bulk sample play a governing role in shaping the inversion layer of 2D charge carriers. It is also clear that it is possible to control the properties of such a layer by means of an external voltage.

This work was supported in part by a grant from the Soros Foundation awarded by the American Physical Society.

[1] R. Herrmann *et al.*, Solid State Commun. **52**, 843 (1984).
[2] G. Grabecki *et al.*, Appl. Phys. Lett. **45**, 1214 (1984).
[3] B. M. Vul and E. Y. Zavaritskaya, Zh. Eksp. Teor. Fiz. **76**, 1089 (1979) [Sov. Phys. JETP **49**, 551 (1979)].
[4] W. Kraak *et al.*, Phys Status Solidi B **161**, 613 (1990).
[5] W. Kraak *et al.*, Superlattices and Microstructures **9**, 471 (1991).
[6] N. B. Brandt *et al.*, Zh. Eksp. Teor. Fiz. **89**, 2257 (1985) [Sov. Phys. JETP **62**, 1303 (1985)].
[7] A. V. Germanenko *et al.*, Fiz. Tekh. Poluprovodn. **23**, 796 (1989) [Sov. Phys. Semicond. **23**, 500 (1989)].
[8] S. G. Gasan-zade *et al.*, Fiz. Tekh. Poluprovodn. **21**, 2066 (1987) [Sov. Phys. Semicond. **21**, 1252 (1987)].
[9] L. A. Bovina *et al.*, Zh. Eksp. Teor. Fiz. **84**, 1453 (1983) [Sov. Phys. JETP **57**, 845 (1983)].
[10] G. Gobsch *et al.*, J. Phys. (Paris) **50**, 283 (1989).
[11] R. Herrmann *et al.*, Phys. Status Solidi B **135**, 423 (1986).

Translated by D. Parsons